Research Square

Preprints are preliminary reports that have not undergone peer review.
They should not be considered conclusive, used to inform clinical practice,
or referenced by the media as validated information.

ALPK2 promotes cell growth via the AP-1 axis in YAP/TAZ-activated oral squamous cell carcinoma

Yume Ueda
Hiroshima University
Nanako Kataoka
Hiroshima University Hospital
Kento Okamoto
Hiroshima University
Kai Omachi
Hiroshima University
Yuga □aeda
Hiroshima University
Yukina Kobayashi
Hiroshima University Hospital
Mikihito Kajiya
Hiroshima University Hospital
Souichi Yanamoto
Hiroshima University
Toshinori Ando
toando19@hiroshima-u.ac.jp
Hiroshima University

Article

Keywords:

Posted Date: July 28th, 2026

DOI: https://doi.org/10.21203/rs.3.rs-10496503/v1

License: This work is licensed under a Creative Commons Attribution 4.0 International License.
Read Full License

Additional Declarations: No competing interests reported.

Abstract

Background

Aberrant activation of YAP/TAZ, the effectors of the Hippo pathway, is involved in the proliferation and progression of oral squamous cell carcinoma (OSCC). However, many aspects of the tumor-promoting mechanisms associated with YAP/TAZ activation remain unclear. In this study, we aimed to identify the key proliferation-asssociated genes regulated by YAP/TAZ in OSCC.

Methods

Cell culture, western blot assays, RNA-seq analysis, knockdown experiments, phosphoproteomic analysis, and gene set enrichment analyses were performed to examine and validate the YAP/TAZ-regulated proliferation-associated genes in OSCC.

Results

RNA-seq analysis indicated alpha-protein kinase 2 (ALPK2) upregulation upon YAP/TAZ activation. YAP/TAZ-related genes were significantly enriched in the ALPK2 high-expression groups of cancer cell lines and tissues. Further, ALPK2 KD significantly inhibited the proliferation of YAP/TAZ-activated OSCC and EGFR-mutant lung adenocarcinoma cells. Phosphoproteomic and RNA-seq analyses revealed altered expression of MTA2-, and AP-1-related molecules, suggesting that these signaling pathways may be involved in the tumor-promoting effects of ALPK2.

Conclusions

ALPK2 may contribute to cell proliferation in YAP/TAZ-activated cancers and the MTA2 and AP-1-related signaling pathways may be involved in its function. Overall, ALPK2 may serve as a novel therapeutic target in OSCC, and its molecular mechanisms need to be examined further.

INTRODUCTION

GLOBOCAN estimates from the International Agency for Research on Cancer (IARC), indicate that oral cancer accounts for approximately 377,000 new cases and 177,000 deaths annually worldwide [1], the majority of which are attributed to OSCC [2]. The incidence of OSCC has been increasing with population aging [1,3]. Although surgical resection remains the primary treatment modality [2], it often results in substantial aesthetics and oral function impairments, thereby adversely affecting the patients' quality of life and psychological well-being [4,5]. Furthermore, patients with advanced, recurrent, or metastatic

disease have poor prognosis [2], underscoring the need for elucidating the underlying molecular mechanisms and developing novel therapeutic strategies.

The Hippo signaling pathway, a highly conserved regulator of organ size and tissue homeostasis [6,7], plays a critical role in tumorigenesis [8]. This pathway comprisesa kinase cascade involving mammalian STE20-like kinase 1 and 2 (MST1/2) and large tumor suppressor 1 and 2 (LATS1/2), together with their adaptor proteins salvador homologue 1 (SAV1) and MOB kinase activator 1A and 1B (MOB1), as well as the transcriptional co-activators YAP and TAZ [9]. Upon Hippo pathway activation, MST1/2 and LATS1/2 are sequentially phosphorylated, leading to YAP phosphorylation at multiple serine residues by LATS1/2 [10]. Phosphorylated YAP binds to 14-3-3 proteins and is retained in the cytoplasm [10] or undergoes ubiquitin-mediated proteasomal degradation [11]. In contrast, upon Hippo pathway inactivation, YAP is dephosphorylated and translocated into the nucleus, where it interacts with TEAD transcription factors [12] to induce the expression of proliferation-related genes such as *connective tissue growth factor* (*CTGF*) and *cysteine-rich angiogenic inducer 61* (*CYR61*) [13].

Aberrant YAP/TAZ activation has been widely observed in various cancers, including OSCC [14,15]. Overexpression of the secreted protein tissue inhibitor of metalloproteinase-1 (TIMP-1) [16] and gene amplification of the receptor tyrosine kinase (RTK) epidermal growth factor receptor (EGFR) are known to constitutively activate YAP/TAZ through inactivation of LATS1/2 in OSCC [17]. Further, AXL, another RTK, forms heterodimers with EGFR, thereby activating YAP/TAZ signaling and conferring resistance to EGFR-targeted therapies [18]. Furthermore, RBM39, an RNA-binding protein, enhances the transcriptional activity of activated YAP/TAZ that has translocated into the nucleus [19]. However, the full spectrum of transcriptional programs regulated by YAP/TAZ in OSCC remains largely unclear.

ALPK2 is a cytoplasmic serine/threonine kinase belonging to the atypical alpha-kinase family [20]. Unlike conventional kinases, ALPK2 contains a unique alpha-kinase domain that recognizes alpha-helical structures in its substrates [21]. ALPK2 promotes cell proliferation in ovarian cancer [22], renal cell carcinoma [23] and bladder cancer [24], and its associations with the PI3K/AKT signaling pathways [22,23] and DEPDC1A (DEP domain containing 1A) [24] have been reported as downstream signaling pathways in these tumors; however, the detailed functions and downstream signaling pathways of ALPK2 remain unclear.

In OSCC, we focused on metastasis-associated protein 2 (MTA2) and activator protein-1 (AP-1) as downstream signaling molecules of ALPK2. MTA2 is a core component of the Nucleosome Remodeling and Deacetylase (NuRD) complex, which possesses both ATP-dependent chromatin remodeling and histone deacetylase activities [25,26]. MTA2 promotes tumor growth in many cancer types [27–29], and its high expression has been strongly correlated with enhanced metastatic potential [30,31] and poor prognosis [32,33]. Y-box binding protein-1 (YB-1) is a multifunctional nucleic acid-binding protein [34] that regulates the transcription of proliferation- and drug resistance-related genes [35]. Furthermore, as an

oncoprotein, nuclear expression of YB-1 is considered an independent biomarker of cancer progression, malignancy, epithelial-mesenchymal transition (EMT), and widespread treatment resistance [35,36]. AP-1 is a transcription factor complex composed of the Jun and Fos families; its abnormal activation is involved in promoting cancer onset, progression, and metastasis of cancer [37].

In this study, we aimed to identify the key proliferation-associated genes regulated by YAP/TAZ in OSCC. We identified ALPK2 as a novel YAP/TAZ-regulated gene and clarified that the ALPK2-MTA2-AP-1 axis plays an important role on proliferation of OSCC. By elucidating the ALPK2-centered regulatory network, this study is expected to advance our understanding of OSCC pathogenesis and to provide a foundation for developing novel therapeutic targets and treatment strategies.

MATERIALS AND METHODS

Antibodies and reagents

Anti-pERK1/2 (T202/Y204) (#9101, 1:1000) and anti-ERK1/2 (#4376, 1:1000) were purchased from Cell Signaling Technology (Danvers, MA, USA). Anti-β-actin (#A2228) was purchased from Sigma-Aldrich Inc (Burlington, MA, USA). Anti-FOSL1 (66590-1-Lg, 1:1000) was purchased from Proteintech (Rosemont, IL, USA). Trametinib DMSO solvate (GSK1120212B) was purchased from Selleck (Houston, TX, USA).

Cell culture and transfection

CAL27 and WSU-HN6 cells were kindly provided by Professor J Silvio Gutkind. HCC827 and PC-9 cells were kindly provided by Professor Susumu Kobayashi. Cell line identities were verified by STR profiling and lack of mycoplasma infection was also confirmed. CAL27 and WSU-HN6 cells were cultured in DMEM (D-6429, Sigma-Aldrich Inc.). HCC827 and PC-9 cells were cultured in RPMI 1640 (30264-56, Nacalai Tesque, Kyoto, Japan) supplemented with 5% GlutaMAX™ Supplement (35050061, Gibco™). Each medium was supplemented with 10% FBS (Sigma-Aldrich Inc.) and 1% penicillin/streptomycin.

Western blotting

For western blotting, cells were harvested after two rinses with cold PBS and lysed in RIPA buffer (50 mM Tis-HCl, 150 mM NaCl, 1 mM EDTA, and 1% NP 40), supplemented with PhosSTOP™ and cOmplete™ (Basel, Switzerland, Roche). The lysate was sonicated three times for 5 s each, incubated for 15 min on ice, and then centrifuged for 15 min. The protein concentration of the supernatant was measured. Equal amounts of protein were loaded for SDS-PAGE and transferred to the membranes. The membranes were blocked with 3% BSA in TBS-T buffer for 20 min. The membranes were then incubated with primary antibodies diluted with 3% BSA or 5% non-fat milk in TBS-T buffer for 2 h at room temperature. After washing thrice with TBS-T buffer, the membranes were incubated with secondary antibodies (HRP-conjugated goat anti-mouse or anti-rabbit IgG at 1:3000, Cell Signaling Technology) diluted with 5% non-

fat milk in TBS-T buffer for 1 h at room temperature. Western Lightning Pro, Chemiluminescent Substrate (Revvity, Waltham, MA, USA) was used for detection.

RNA isolation and real-time PCR

RNA was extracted using the RNeasy Mini Kit following the manufacturer's instructions (#74104, Qiagen, Hilden, Germany). One microgram of total RNA was used for cDNA synthesis using the Super Script™ IV VILO™ Master Mix cDNA synthesis kit. Real-time PCR was performed using the Fast SYBR™ Green Master Mix (#4385612, Applied Biosystems). The experiment was performed with N = 3. Reactions were performed in triplicate and the gene expression data were relatively quantified using the $2^{-\Delta\Delta Ct}$ method. The following primers were as follows: GAPDH F: 5'-GAGTCAACGGATTTGGTCGT-3', R: TTGATTTTGGAGGGATCTCG-3'; and ALPK2 F: 5'-TCCGAAGGACCAGGGACTCTAT-3', R: CGGTGAACCCCTTCTCCAAA – 3'.

Cell proliferation (cell viability assay)

Cells were seeded in 96 well plates at 5000 cells per well and treated with reagents for 3 days. Cell titer blue reagent™ (#G8081, Promega) was applied to the culture medium, and incubated for 2 h, and the absorbance was then measured using a microplate reader. The experiment was performed with N = 5.

Crystal violet staining

The cells were seeded in 6-well plates. The attached cells were fixed with 4% formalin for 20 min, then stained with 0.5% crystal violet solution containing 20% methanol for 5 min.

Knockdown by siRNA

Cells were transfected with siRNA using the Lipofectamine RNAimax Reagent (Thermo fisher scientific). The siRNAs for FOSL1 (SASI_Hs01_0019_1186) and the negative control (MISSION® siRNA Universal Negative Control #2) were purchased from Sigma Aldrich. The siRNA for ALPK2 (Silencer® Validated siRNA) was purchased from ThermoFisher Scientific.

Lentiviral shRNA vector construction and cell transfection

Stable ALPK2-KD cell lines were established using MISSION® shRNA lentiviral vectors (Sigma-Aldrich, St. Louis, MO, USA) based on the pLKO.1 backbone. An shRNA targeting human ALPK2 (TRCN0000194883) was used for generating ALPK2 KD cells, and a non-targeting shRNA control (SHC016V) was used as a negative control. Control cells were selected using puromycin, whereas ALPK2 shRNA-transduced cells were selected using G418 (Geneticin) to establish stable cell lines. Knockdown efficiency was confirmed by quantitative real-time PCR (qRT-PCR).

RNA-seq

Total RNA was extracted from WT and LATS1/2 knockout (KO) CAL27 cells, as well as siControl and siALPK2 in WSU-HN6 cells (N = 3). RNA-seq libraries were prepared using the TruSeq Stranded mRNA LT Sample Prep Kit and sequenced on the Illumina NovaSeq X platform. For each sample, paired-end sequencing reads were mapped to the GRCh38 human reference genome using HISAT2 version 2.1.0. Transcript assembly and abundance quantification were computed using StringTie version 2.1.3b. Differential gene expression analysis was performed using DESeq2 version 1.46.0 using a parametric fit. MORPHEUS (https://software.broadinstitute.org/morpheus) was used to generate heat maps.

Phosphoproteomic analysis

WSU-HN6 cells transfected with siControl and siALPK2 were harvested and lysed in lysis buffer containing protease and phosphatase inhibitors. Protein samples were digested with trypsin, and phosphopeptides were enriched using IMAC. Shotgun phosphoproteomic analysis was performed using liquid chromatography–tandem mass spectrometry (LC-MS/MS) on a Q-Exactive Plus mass spectrometer coupled with a Dionex UltiMate 3000 system. Raw MS/MS spectra were processed using Scaffold software and searched against the UniProt human protein database. Quantitative phosphoproteomic analysis was performed using a label-free quantification (LFQ) method based on intensity-based absolute quantification (iBAQ). Differentially phosphorylated proteins were identified using the following criteria: $P < 0.05$.

Gene set enrichment analysis (GSEA)

We analyzed the Cancer Cell Line encyclopedia (CCLE) and the Cancer Genome Atlas (TCGA) datasets using gene set enrichment analysis (GSEA) (Broad Institute, http://software.broadinstitute.org/gsea/index.jsp) with 1000 permutations, “Pearson” metric of RNA-seq read counts per gene and a gene set size filter of 15–500. The “C6” gene set database from MSigDB was spiked with “ZHANG: TEAD-YAP/TAZ”.

Statistical analysis

All data were analyzed using GraphPad Prism version 9 (GraphPad Software, CA, USA). The data were analyzed using the Student’s t-test (two sided) and analysis of variance (ANOVA) with the Tukey-Kramer post hoc test or as indicated in the figure legends. All experiments were independently repeated three times, with similar results.

For all volcano plots, red dots indicate features meeting both the fold-change and statistical significance thresholds, green dots indicate features meeting only the fold-change threshold, blue dots indicate features meeting only the statistical significance threshold, and gray dots indicate features meeting neither threshold.

Data availability

Raw and processed RNA-seq data were deposited in the NCBI Gene Expression Omnibus (GEO) and can be accessed under the GEO Series Accession Number GSE (not yet). The CCLE data set is available online (https://portals.broadinstitute.org/ccle) and the TCGA data is

available from c-BioPortal (https://www.cbioportal.org/). The datasets generated during and/or analyzed during the current study are available from the corresponding author on reasonable request.

RESULTS

ALPK2 is a YAP/TAZ-regulated gene

We previously generated LATS1/2 KO CAL27 cells, a human HNSCC cell line. LATS1/2 KO CAL27 cells showed YAP dephosphorylation and no change in ERK phosphorylation (Supplementary Fig. 1A). We then performed RNA sequencing using these cells and WT CAL27 cells and among the differentially expressed genes (DEGs), we focused on kinases. Significantly upregulated kinases from the DEGs in LATS1/2 KO CAL27 cells were extracted and sorted by descending fold change (Fig. 1A). We identified ALPK2 as the kinase showing the highest expression among kinases (Fig. 1A).

To determine whether ALPK2 expression correlates with YAP/TAZ activation in actual cancer cell lines or tissues, we performed GSEA using RNA sequencing data from the CCLE (including 1072 cell lines derived from various organs) and the TCGA PanCancer Atlas (including tissue samples from 517 patients with HNSCC). ALPK2-enriched YAP-targeted gene sets included ZHANG: TEAD-YAP/TAZ, DUPONT: YAP and CORDENONSI_YAP_CONSERVED_SIGNATURE (Figs. 1B, C). Collectively, these results indicate that ALPK2 is significantly upregulated in YAP/TAZ-activated OSCC and is positively correlated with YAP/TAZ activity in publicly available datasets of cancer cell lines and tissues.

ALPK2 knockdown inhibits cell proliferation

Two OSCC cell lines demonstrating YAP/TAZ activation—WSU-HN6 cells harboring EGFR gene amplification and LATS1/2 KO CAL27 cells—were transfected with siRNA to knockdown ALPK2. Crystal violet staining showed that ALPK2 KD significantly inhibited cell growth in both cell lines (Fig. 2A). Similar results were confirmed in the cell viability results (Fig. 2B). We established shALPK2-transduced WSU-HN6 cells with stable ALPK2 KD. In these cells, ALPK2 expression was reduced, and cell proliferation was inhibited (Figs. 2C, D).

We also conducted experiments using lung adenocarcinoma (LUAC) cells harboring EGFR gene-activating mutations. We performed qPCR using WT HCC827 cells and LATS1/2KO HCC827 cells with highly activated YAP/TAZ. ALPK2 expression was significantly increased in LATS1/2KO HCC827 cells (Fig. 2E). PC-9 cells were transfected with ALPK2-targeting siRNA. ALPK2 mRNA expression was decreased in siALPK2-transfected PC-9 cells compared with siControl PC-9 cells. (Fig. 2F). Furthermore,

ALPK2 KD significantly suppressed PC-9 cell viability. (Fig. 2G, H). These findings suggest that ALPK2 plays an important role in tumor cell proliferation in both OSCC and LUAC.

Exploring the Downstream Signaling Pathway of ALPK2

Previous studies have suggested PI3K/AKT signaling pathway involvement in ALPK2-mediated tumor progression in ovarian cancer [22] and renal cell carcinoma [23]. Therefore, we investigated whether ALPK2 KD affects the AKT/mTOR signaling pathway in OSCC cells by evaluating the phosphorylation levels of AKT and S6. However, transfecting WSU-HN6 cells with siALPK2 did not show any changes in phosphorylation, thus reflecting AKT and S6 activation in western blots (Supplementary Fig. 1B). As a signaling pathway different than that previously reported may be involved, we performed phosphoproteomic analysis using siControl and siALPK2 in WSU-HN6 cells. Factors such as MTA2 were identified as showing a significant reduction of phosphorylation upon ALPK2 KD (Fig. 3A). MTA2 exerts a tumor-suppressive effect by regulating AP-1 via YB1 [31]. Therefore, we examined pYB1 (S102) but found no change in the phosphorylation level by siALPK2 transfection in WSU-HN6 cells (Supplementary Fig. 2A).

To further investigate the downstream signaling pathway of the ALPK2-MTA2 axis, we performed RNA sequencing and GSEA to determine the genes altered by ALPK2 KD in WSU-HN6 cells. ALPK2 knockdown led to the accumulation of MYC activation-related genes (MYC_UP. V1_UP) (Supplementary Fig. 2B). Proteins likely to fluctuate in coordination with MYC include ERK, PI3K [38,39], and AP-1 [14], which consists of JUN and FOS. The volcano plot shows that siALPK2 transfection in WSU-HN6 cells significantly reduces FOSL1 expression (Fig. 3B). The heatmap shows the expression of the JUN and FOS family. Although ALPK2 knockdown reduced the expression of several genes, the most significantly downregulated gene was FOSL1 (Fig. 3C). However, the heatmap generated from RNA-seq data of the WT and LATS1/2 KO CAL27 cells showed increased expression of FOSL1 and JUN in LATS1/2 KO cells (Fig. 3D). Western blot analysis revealed that ALPK2 KD reduced FOSL1 expression in all the cell lines used: WHU-HN6 cells, LATS1/2KO CAL27 cells, PC-9 cells, and LATS1/2KO HCC827 cells (Fig. 3E, F and Supplementary Fig. 3). Taken together, these findings suggest that FOSL1 may act downstream of ALPK2 through MTA2.

FOSL1 contributes to the proliferation of YAP/TAZ-activated OSCC cells and their sensitivity to trametinib

As MAPK signaling was altered by ALPK2 KD, we performed a functional analysis using trametinib, a MEK1/2 inhibitor. Trametinib inhibits downstream ERK phosphorylation [40]. Immunoblot analysis revealed inhibition of pERK and its downstream target FOSL1 in the trametinib-treated group. LATS1/2KO CAL27 cells showed increased FOSL1 band intensity relative to WT CAL27 cells (Fig. 4A). Further, LATS1/2KO CAL27 cells with highly activated YAP/TAZ showed decreased IC_{50} of trametinib and increased sensitivity to MEK inhibition (Fig. 4B). We transfected WSU-HN6 cells with siFOSL1, and using western blot, confirmed that FOSL1 expression was suppressed (Fig. 4C). Cell growth was significantly reduced following FOSL1 KD, as determined by crystal violet staining (Fig. 4D).

These findings indicate that FOSL1 promotes the proliferation of YAP/TAZ-activated OSCC cells and is associated with their increased sensitivity to trametinib.

DISCUSSION

To our knowledge, this study is the first to demonstrate the potential involvement of ALPK2 in OSCC progression via the YAP/TAZ pathway and to suggest a link with the MTA2-AP-1 signaling axis (Fig. 4C).

ALPK2 was firstly reported by Ryazanov et al. in 1999 [20]; subsequently, in 2018, ALPK2 was found to promote cardiomyocyte differentiation by suppressing the Wnt/β-catenin signaling pathway during zebrafish heart development [41]. Further, it has been found to function as an oncoprotein in various types of cancer. In 2024, ALPK2 has been reported to maintain cardiac diastolic function by directly phosphorylating the Ser283 residue of tropomyosin 1 (TPM1) [42]. However, the specific sites of direct phosphorylation by ALPK2 in cancer research have not been identified to date.

In head and neck cancers, including OSCC, *YAP1* gene amplification and *FAT1* loss or mutations cause persistent YAP/TAZ accumulation in the nucleus, thereby promoting tumor growth [17,43]. High ALPK2 expression levels were observed in YAP/TAZ-activated OSCC and LUAC (Fig. 1A and Fig. 2D), and ALPK2 KD was found to significantly inhibit tumor growth (Fig. 2). This is consistent with reports indicating that ALPK2 functions as a tumor-promoting factor in ovarian cancer [22], renal cell carcinoma [23] and bladder cancer [24]. ALPK2 is also a poor prognostic factor in endometrial cancer [44]. Overall, ALPK2 is believed to play a key role in YAP/TAZ-mediated tumor proliferation.

We identified involvement of the MTA2-AP-1 pathway in ALPK2 downstream signaling (Fig. 3). MTA2 regulates AP-1 activity through the phosphorylation of YB-1, thus driving the cell proliferation program [31]. Further, under MTA2 KD conditions, AP-1 is suppressed owing to an increase in pYB-1, leading to reduced invasive capacity [31]; however, in the present study, pYB-1 (Ser102) levels were not changed in the presence of decreased pMTA2. Although phosphorylation at Ser102 has been widely associated with YB-1 activation, phosphorylation at Ser209 is reported to inhibit its nuclear translocation, suggesting that phosphorylation at different residues leads to different biological effects [45]. Therefore, altered phosphorylation of Ser102 alone may not fully reflect the functional state of YB-1; the exact mechanism linking MTA2 phosphorylation to YB-1 signaling in OSCC thus remains unclear necessitating further detailed investigations, including Ser209. is needed. The involvement of the PI3K-AKT pathway in ovarian cancer [22] and renal cell carcinoma [23], and of DEPDC1A in bladder cancer [24], has been reported in the downstream signaling of ALPK2. Therefore, multiple signaling pathways may be involved downstream of ALPK2.

In OSCC, YAP/TAZ, which has translocated into the nucleus because of Hippo pathway disruption, is known to promote tumor proliferation [46]. However, YAP/TAZ are co-transcription factors and lack catalytic active sites, making them difficult to directly inhibit using small-molecule compounds [47,48].

MST1/2 and LATS1/2, which are upstream of the Hippo pathway, are common kinase targets for drug development; however, as they function as tumor suppressors, their inhibition activates YAP/TAZ, which has the opposite effect [49,50]. Consequently, TEAD-targeted drug development has been proposed, and TEAD inhibitors such as K-975 have demonstrated antitumor effects against YAP-dependent malignancies in preclinical trials [51], while VT3989 has shown promising clinical efficacy against mesothelioma in Phase 1/2 clinical trials [52].

Resistance to EGFR inhibitors in OSCC is a serious challenge. The mechanism is known to involve the RTK receptor AXL forming a heterodimer with EGFR, which, through MOB1, inactivates LATS1/2, thereby reactivating YAP [18]; furthermore, the reactivated YAP strongly induces the expression of AP-1, Bcl-2 [53], and MMP12 [54]. ALPK2, identified in this study, is a non-typical kinase, facilitating development of small-molecule compounds targeting its active site [55]. As ALPK2 is involved in regulating YAP/TAZ-related signaling, developing ALPK2-targeted inhibitors may represent a promising therapeutic strategy for OSCC. However, many aspects of the structural features of ALPK2—including its autophosphorylation sites—and its kinase activity remain unclear, and further analysis is needed to develop inhibitors. In future, ALPK2 inhibitors may become a treatment option that can be used in combination with other molecularly targeted therapies.

Although this study identified MTA2 as a downstream target of ALPK2, some limitations remain; we have not yet been able to determine in detail, through in vitro kinase assays or co-immunoprecipitation (Co-IP), whether ALPK2 phosphorylates MTA2 directly or through an indirect mechanism involving other components of the NuRD complex. Our findings suggest the involvement of MTA2 and YB-1 in ALPK2-mediated tumor-promoting signaling. Nevertheless, the causal relationship among ALPK2, MTA2, and YB-1 remains to be fully established. Further mechanistic studies are required to clarify how ALPK2 regulates YB-1 signaling. Another limitation is that although ALPK2 expression was associated with YAP/TAZ activation, whether ALPK2 is directly regulated by the YAP/TAZ–TEAD transcriptional complex remains unclear. In particular, further investigation using methods such as chromatin immunoprecipitation analysis is needed to determine whether the YAP/TAZ–TEAD complex directly binds to the ALPK2 promoter or enhancer region to regulate transcription. Further, even though ALPK2 may be a promising therapeutic target for OSCC, the risk of side effects leading to impaired cardiac diastolic function—such as heart failure with preserved ejection fraction (HFpEF)—cannot be ruled out with systemic inhibition, particularly in elderly patients and those with a history of heart disease [42]. For this reason, future inhibitor development will require tumor-specific delivery strategies.

In conclusion, we have demonstrated that YAP/TAZ, activated by various genetic abnormalities in OSCC and EGFR-activating mutation-positive LUAC, enhances ALPK2 transcription. We suggested that downstream of ALPK2, AP-1 transcription is induced via MTA2, thereby promoting tumor growth. Considering the limited therapeutic strategies targeting YAP/TAZ signaling, our findings suggest that ALPK2 may represent a novel therapeutic vulnerability in YAP/TAZ-active OSCC. By elucidating the downstream signaling of ALPK2 in OSCC in greater detail, we can evaluate ALPK2 as a biomarker and

determine the appropriate indications for Hippo pathway inhibitors and future ALPK2 inhibitors, thus paving the way for precision medicine.

Declarations

Competing interests

All authors declare no conflicts of interest.

Acknowledgements

This work was supported by JSPS JP24K02645, Takeda Science Foundation, the JST HIRAKU-Global program and JST SPRING, Grant Number JPMJSP2132.

Author contributions

Initiated the study: YU, TA

Designed the study and experiments: YU, TA

Performed the genomic analysis: YU, TA, NK, YM

Performed in vitro experiments: YU, TA, KO, NK, KO, YM, YK

Prepared the manuscript: YU, TA, NK, KO, YM, KO, YK, SY, MK

Supervised the project: TA

All authors have discussed the results and reviewed the manuscript.

References

1. Bray, F. *et al.* Global cancer statistics 2022: GLOBOCAN estimates of incidence and mortality worldwide for 36 cancers in 185 countries. *CA Cancer J. Clin.* **74**, 229–263 (2024).
2. Tan, Y. *et al.* Oral squamous cell carcinomas: state of the field and emerging directions. *Int J Oral Sci* **15**, 44 (2023).
3. Mrosk, F. *et al.* The impact of patient age on the oncological prognosis of oral squamous cell carcinoma. *Oral Maxillofac. Surg.* **30** (2026).
4. Bakshi, J., Goyal, A. K. & Saini, J. Quality of Life in Oral Cancer Patients Following Surgical Excision and Flap Reconstruction. *J. Maxillofac. Oral Surg.* **21**, 326–331 (2021).
5. Filippini, D. M. *et al.* Health-related quality of life assessment in head and neck cancer: A systematic review of phase II and III clinical trials. *Heliyon* **10**, e40671 (2024).

6. Harvey, K. F., Pfleger, C. M. & Hariharan, I. K. The Drosophila Mst ortholog, hippo, restricts growth and cell proliferation and promotes apoptosis. *Cell* **114**, 457–467 (2003).
7. Wu, S., Huang, J., Dong, J. & Pan, D. hippo encodes a Ste-20 family protein kinase that restricts cell proliferation and promotes apoptosis in conjunction with salvador and warts. *Cell* **114**, 445–456 (2003).
8. Overholtzer, M. *et al.* Transforming properties of YAP, a candidate oncogene on the chromosome 11q22 amplicon. *Proc. Natl. Acad. Sci. U. S. A.* **103**, 12405–12410 (2006).
9. Dong, J. *et al.* Elucidation of a universal size-control mechanism in Drosophila and mammals. *Cell* **130**, 1120–1133 (2007).
10. Zhao, B. *et al.* Inactivation of YAP oncoprotein by the Hippo pathway is involved in cell contact inhibition and tissue growth control. *Genes Dev.* **21**, 2747–2761 (2007).
11. Zhao, B., Li, L., Tumaneng, K., Wang, C. Y. & Guan, K. L. A coordinated phosphorylation by Lats and CK1 regulates YAP stability through SCF(beta-TRCP). *Genes Dev.* **24**, 72–85 (2010).
12. Vassilev, A., Kaneko, K. J., Shu, H., Zhao, Y. & DePamphilis, M. L. TEAD/TEF transcription factors utilize the activation domain of YAP65, a Src/Yes-associated protein localized in the cytoplasm. *Genes Dev.* **15**, 1229–1241 (2001).
13. Zhao, B. *et al.* TEAD mediates YAP-dependent gene induction and growth control. *Genes Dev.* **22**, 1962–1971 (2008).
14. Zanconato, F. *et al.* Genome-wide association between YAP/TAZ/TEAD and AP-1 at enhancers drives oncogenic growth. *Nat. Cell Biol.* **17**, 1218–1227 (2015).
15. Omori, H. *et al.* YAP1 is a potent driver of the onset and progression of oral squamous cell carcinoma. *Sci Adv* **6**, eaay3324 (2020).
16. Ando, T. *et al.* Tissue inhibitor of metalloproteinase-1 promotes cell proliferation through YAP/TAZ activation in cancer. *Oncogene* **37**, 263–270 (2018).
17. Ando, T. *et al.* EGFR Regulates the Hippo pathway by promoting the tyrosine phosphorylation of MOB1. *Commun Biol* **4**, 1237 (2021).
18. Okamoto, K. *et al.* AXL activates YAP through the EGFR-LATS1/2 axis and confers resistance to EGFR-targeted drugs in head and neck squamous cell carcinoma. *Oncogene* **42**, 2869–2877 (2023).
19. Ando, T. *et al.* YAP/TAZ interacts with RBM39 to confer resistance against indisulam. *Oncogenesis* **13**, 25 (2024).
20. Ryazanov, A. G., Pavur, K. S. & Dorovkov, M. V. Alpha-kinases: a new class of protein kinases with a novel catalytic domain. *Curr. Biol.* **9**, R43–45 (1999).
21. Drennan, D. & Ryazanov, A. G. Alpha-kinases: analysis of the family and comparison with conventional protein kinases. *Prog. Biophys. Mol. Biol.* **85**, 1–32 (2004).
22. Zhu, X., Yan, S., Xiao, S. & Xue, M. Knockdown of ALPK2 inhibits the development and progression of Ovarian Cancer. *Cancer Cell Int.* **20**, 267 (2020).

23. Jiang, J. *et al.* Knockdown of ALPK2 blocks development and progression of renal cell carcinoma. *Exp. Cell Res.* **392**, 112029 (2020).
24. Wang, Y. *et al.* ALPK2 acts as tumor promotor in development of bladder cancer through targeting DEPDC1A. *Cell Death Dis.* **12**, 661 (2021).
25. Xue, Y. *et al.* NURD, a novel complex with both ATP-dependent chromatin-remodeling and histone deacetylase activities. *Mol. Cell* **2**, 851–861 (1998).
26. Zhang, Y., LeRoy, G., Seelig, H. P., Lane, W. S. & Reinberg, D. The dermatomyositis-specific autoantigen Mi2 is a component of a complex containing histone deacetylase and nucleosome remodeling activities. *Cell* **95**, 279–289 (1998).
27. Zhou, C. *et al.* MTA2 enhances colony formation and tumor growth of gastric cancer cells through IL-11. *BMC Cancer* **15**, 343 (2015).
28. Zhou, J. *et al.* P300 binds to and acetylates MTA2 to promote colorectal cancer cells growth. *Biochem. Biophys. Res. Commun.* **444**, 387–390 (2014).
29. Guan, C., Chang, Z., Gu, X. & Liu, R. MTA2 promotes HCC progression through repressing FRMD6, a key upstream component of hippo signaling pathway. *Biochem. Biophys. Res. Commun.* **515**, 112–118 (2019).
30. Zhou, C. *et al.* MTA2 promotes gastric cancer cells invasion and is transcriptionally regulated by Sp1. *Mol. Cancer* **12**, 102 (2013).
31. Lin, C. L. *et al.* MTA2 silencing attenuates the metastatic potential of cervical cancer cells by inhibiting AP1-mediated MMP12 expression via the ASK1/MEK3/p38/YB1 axis. *Cell Death Dis.* **12**, 451 (2021).
32. Liu, Y. P., Shan, B. E., Wang, X. L. & Ma, L. Correlation between MTA2 overexpression and tumour progression in esophageal squamous cell carcinoma. *Exp. Ther. Med.* **3**, 745–749 (2012).
33. Si, W. *et al.* MTA2-mediated inhibition of PTEN leads to pancreatic ductal adenocarcinoma carcinogenicity. *Cell Death Dis.* **10**, 206 (2019).
34. Lasham, A. *et al.* YB-1, the E2F pathway, and regulation of tumor cell growth. *J. Natl. Cancer Inst.* **104**, 133–146 (2012).
35. Maurya, P. K. *et al.* Role of Y Box Protein-1 in cancer: As potential biomarker and novel therapeutic target. *J. Cancer* **8**, 1900–1907 (2017).
36. Kolk, A. *et al.* Expression of Y-box-binding protein YB-1 allows stratification into long- and short-term survivors of head and neck cancer patients. *Br. J. Cancer* **105**, 1864–1873 (2011).
37. Song, D., Lian, Y. & Zhang, L. The potential of activator protein 1 (AP-1) in cancer targeted therapy. *Front. Immunol.* **14**, 1224892 (2023).
38. Lee, T., Yao, G., Nevins, J. & You, L. Sensing and integration of Erk and PI3K signals by Myc. *PLoS Comput. Biol.* **4**, e1000013 (2008).
39. Kress, T. R., Sabo, A. & Amati, B. MYC: connecting selective transcriptional control to global RNA production. *Nat. Rev. Cancer* **15**, 593–607 (2015).

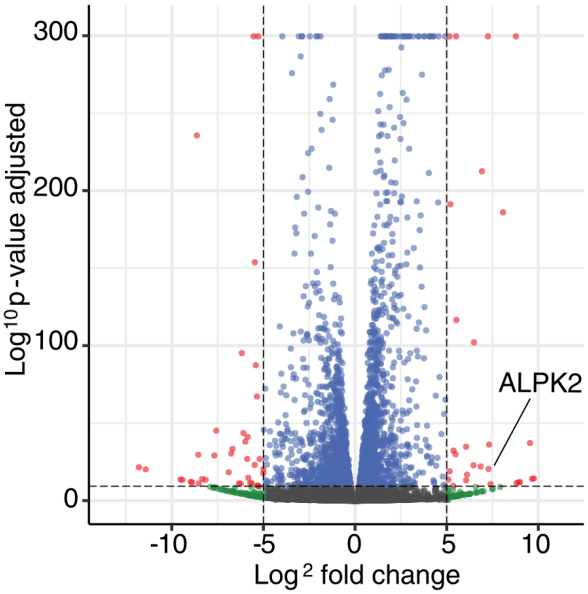
40. Gilmartin, A. G. *et al.* GSK1120212 (JTP-74057) is an inhibitor of MEK activity and activation with favorable pharmacokinetic properties for sustained in vivo pathway inhibition. *Clin. Cancer Res.* **17**, 989–1000 (2011).
41. Hofsteen, P. *et al.* ALPK2 Promotes Cardiogenesis in Zebrafish and Human Pluripotent Stem Cells. *iScience* **2**, 88–100 (2018).
42. Yoshida, T. *et al.* ALPK2 prevents cardiac diastolic dysfunction in heart failure with preserved ejection fraction. *FASEB J.* **38**, e70192 (2024).
43. Martin, D. *et al.* Assembly and activation of the Hippo signalome by FAT1 tumor suppressor. *Nat Commun* **9**, 2372 (2018).
44. Ling, Y., Tao, H., Shan, J. & Wei, W. ALPK2 could serve as a prognostic biomarker for patients with uterine corpus endometrial carcinoma. *Asian J. Surg.* **48**, 6825–6827 (2025).
45. Sogorina, E. M. *et al.* YB-1 Phosphorylation at Serine 209 Inhibits Its Nuclear Translocation. *Int. J. Mol. Sci.* **23** (2021).
46. Ando, T. *et al.* Integrating Genetic Alterations and the Hippo Pathway in Head and Neck Squamous Cell Carcinoma for Future Precision Medicine. *J Pers Med* **12** (2022).
47. Tang, T. T. *et al.* Small Molecule Inhibitors of TEAD Auto-palmitoylation Selectively Inhibit Proliferation and Tumor Growth of NF2-deficient Mesothelioma. *Mol. Cancer Ther.* **20**, 986–998 (2021).
48. Harvey, K. F. & Tang, T. T. Targeting the Hippo pathway in cancer. *Nat Rev Drug Discov* **24**, 852–869 (2025).
49. Hao, Y., Chun, A., Cheung, K., Rashidi, B. & Yang, X. Tumor suppressor LATS1 is a negative regulator of oncogene YAP. *J. Biol. Chem.* **283**, 5496–5509 (2008).
50. Zhou, D. *et al.* Mst1 and Mst2 maintain hepatocyte quiescence and suppress hepatocellular carcinoma development through inactivation of the Yap1 oncogene. *Cancer Cell* **16**, 425–438 (2009).
51. Kaneda, A. *et al.* The novel potent TEAD inhibitor, K-975, inhibits YAP1/TAZ-TEAD protein-protein interactions and exerts an anti-tumor effect on malignant pleural mesothelioma. *Am. J. Cancer Res.* **10**, 4399–4415 (2020).
52. Yap, T. A. *et al.* YAP/TEAD inhibitor VT3989 in solid tumors: a phase 1/2 trial. *Nat. Med.* **31**, 4281–4290 (2025).
53. Alam, M. *et al.* The elevated activation of NFkappaB and AP-1 is correlated with differential regulation of Bcl-2 and associated with oral squamous cell carcinoma progression and resistance. *Clin. Oral Investig.* **21**, 2721–2731 (2017).
54. Samuel, S., Twizere, J. C. & Bernstein, L. R. YB-1 represses AP1-dependent gene transactivation and interacts with an AP-1 DNA sequence. *Biochem. J.* **388**, 921–928 (2005).
55. Middelbeek, J., Clark, K., Venselaar, H., Huynen, M. A. & van Leeuwen, F. N. The alpha-kinase family: an exceptional branch on the protein kinase tree. *Cell. Mol. Life Sci.* **67**, 875–890 (2010).

Figures

A

Rank	Gene Signatures	Fold change	Types of kinases
1	ALPK2	7.3	STPKs
2	PRKCG	5.9	STPKs
3	FLT1	3.5	TPKs
4	PDGFRB	3	TPKs
5	EPHA3	2.9	TPKs
6	INSR	2.9	TPKs
7	DDR2	2.8	TPKs
8	CDKL2	2.2	STPKs
9	SGK1	2	STPKs
10	EPHB1	1.9	TPKs

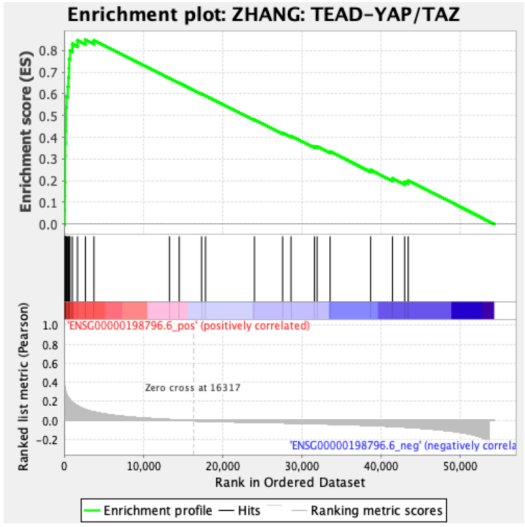
STPKs : Serin/Threonine Protein Kinase
TPKs : Tyrosine Protein Kinase



B

Enrichment analysis of ALPK2 in CCLE (N=1739)

Rank	Gene Signatures	NES	NOM p-val	FDR q-val
1	BMI1_DN_MEL18_DN.V1_UP	2.31	0.000	0.000
2	CAHOY_ASTROGLIAL	2.29	0.000	0.000
3	MEL18_DN.V1_UP	2.23	0.000	0.000
4	ZHANG: TEAD-YAP/TAZ	2.22	0.000	0.000
5	BMI1_DN.V1_UP	2.16	0.000	0.001
6	DUPONT: YAP	2.14	0.000	0.002
7	CORDENONSI_YAP_ CONSERVED_SIGNATURE	2.07	0.000	0.006
8	ESC_V6.5_UP_EARLY.V1_DN	2.00	0.000	0.014
9	EGFR_UP.V1_UP	1.97	0.003	0.027
10	RB_DN.V1_DN	1.95	0.000	0.033



C

Enrichment analysis of ALPK2 in TCGA, PanCancer (N=527)

Rank	Gene Signatures	NES	NOM p-val	FDR q-val
38	ZHANG: TEAD-YAP/TAZ	1.92	0.002	0.005
72	DUPONT: YAP	1.75	0.010	0.014
74	CORDENONSI_YAP_ CONSERVED_SIGNATURE	1.75	0.014	0.015

Figure 1

ALPK2 is positively correlated with YAP/TAZ activation in OSCC

(A) The table lists the kinases whose expression levels were significantly increased by LATS1/2 KO, as identified from the RNA-seq results of WT and LATS1/2KO CAL27 cells. Volcano plot of RNA-seq analysis comparing WT and LATS1/2KO CAL27 cells. Genes with adjusted P<0.05 were considered significantly differentially expressed. ALPK2 is highlighted. (B, C) Gene set enrichment analysis (GSEA) using the RNA-seq data from the cancer cell line encyclopedia (CCLE) and the Cancer Genome Atlas (TCGA) revealed that ALPK2 expression was enriched in YAP/TAZ-target gene sets. Enrichment plots of ZHANG□TEAD-YAP/TAZ signature gene sets for ALPK2.

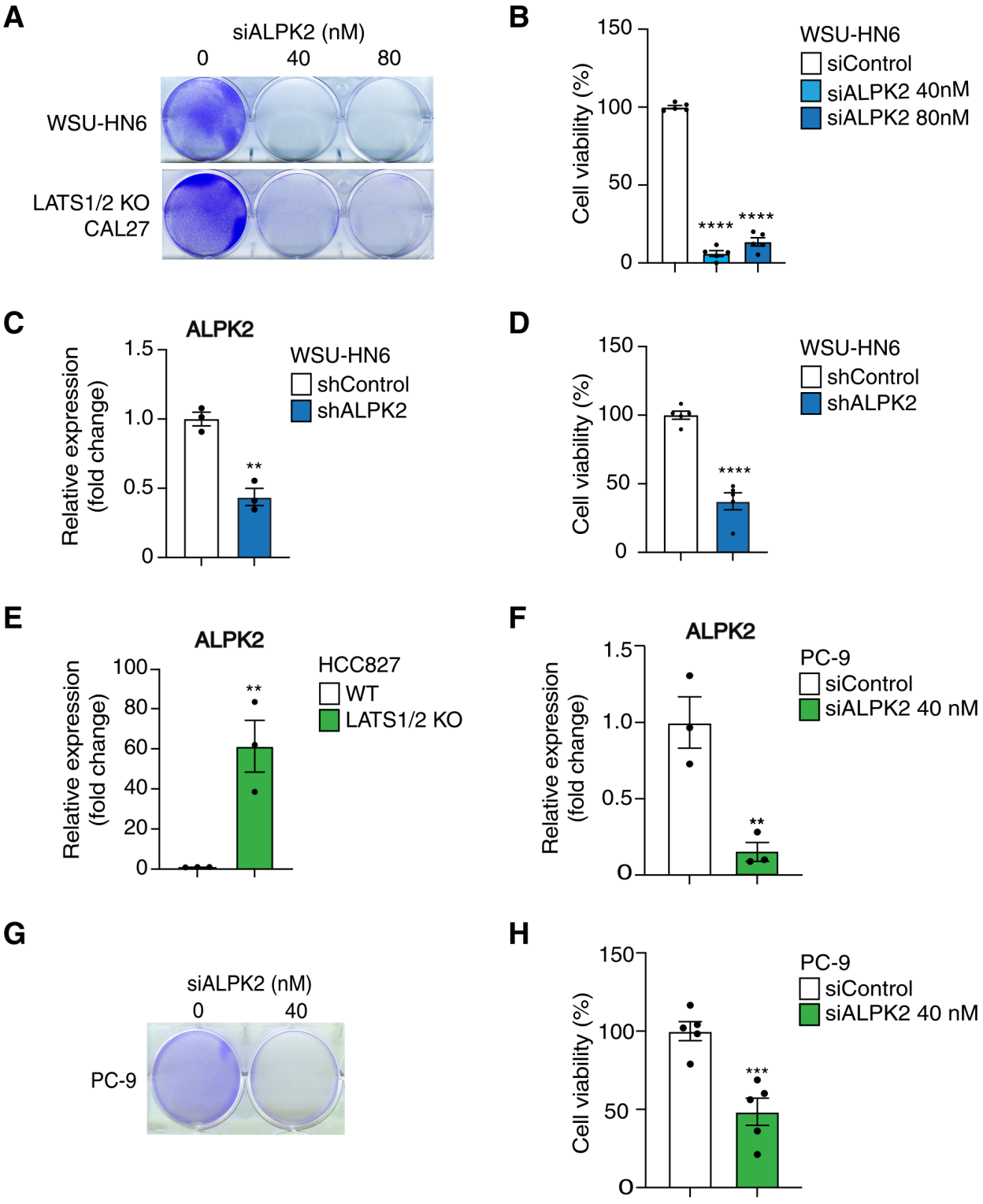


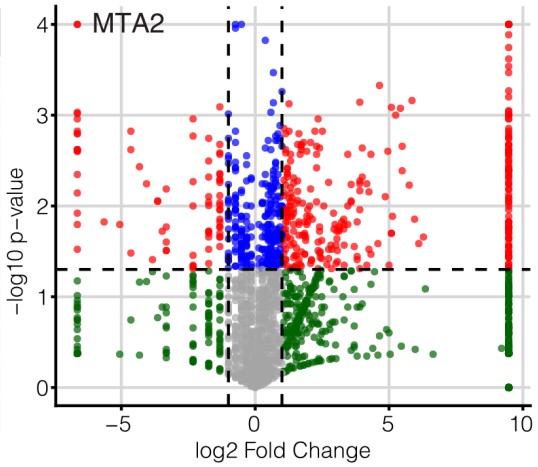
Figure 2

ALPK2 is involved in the proliferation of YAP/TAZ-activated OSCC and LUAC

(A) Crystal violet staining of siALPK2 or siControl in WSU-HN6 and LATS1/2 KO CAL27 cells. (B) Graph of cell viability in WSU-HN6 cells transfected with siALPK2 using the cell titer-blue cell viability assay. (C) The relative mRNA expression levels of ALPK2 in shALPK2-transduced WSU-HN6 cells were measured. Expression levels were normalized against GAPDH and expressed as relative values compared to shControl-transduced WSU-HN6 cells. (D) Graph of cell viability in shALPK2-transduced WSU-HN6 cells using the cell titer-blue cell viability assay. (E) The relative ALPK2 mRNA expression levels in LATS1/2KO HCC827 cells were determined by qPCR and are presented as fold change relative to WT HCC827 cells. (F) The relative ALPK2 mRNA expression levels in siALPK2-transfected PC-9 cells were determined by qPCR and are presented as fold change relative to the siControl group. (G) Crystal violet staining of siALPK2 and siControl in PC-9 cells. (H) Graph of cell viability in PC-9 cells transfected with siALPK2 using the cell titer-blue cell viability assay. Data are presented as mean ± SD. Statistical significance was determined using Student's *t*-test for (C-F and H) and one-way ANOVA followed by Tukey–Kramer post hoc test for (B). (B-F and H): ****P < 0.0001, ***P < 0.001, **P < 0.01. (B) *versus siControl.

A

Rank	Protein	Mean Ctrl iBAQ	Mean KD iBAQ	p-value
1	**MTA2**	883870	ND	< 0.00010
2	LPIN3	1208200	ND	< 0.00010
3	VRK3	175210	ND	0.00093
4	PALS1	606725	ND	0.00096
5	UBTF	914825	ND	0.0011
6	PRPF8	233315	ND	0.0015
7	RPLP0P6	598795	ND	0.0016
8	EMSY	392660	ND	0.0016
9	NOPCHANP1	297765	ND	0.0024
10	PRPF13	657750	ND	0.0024



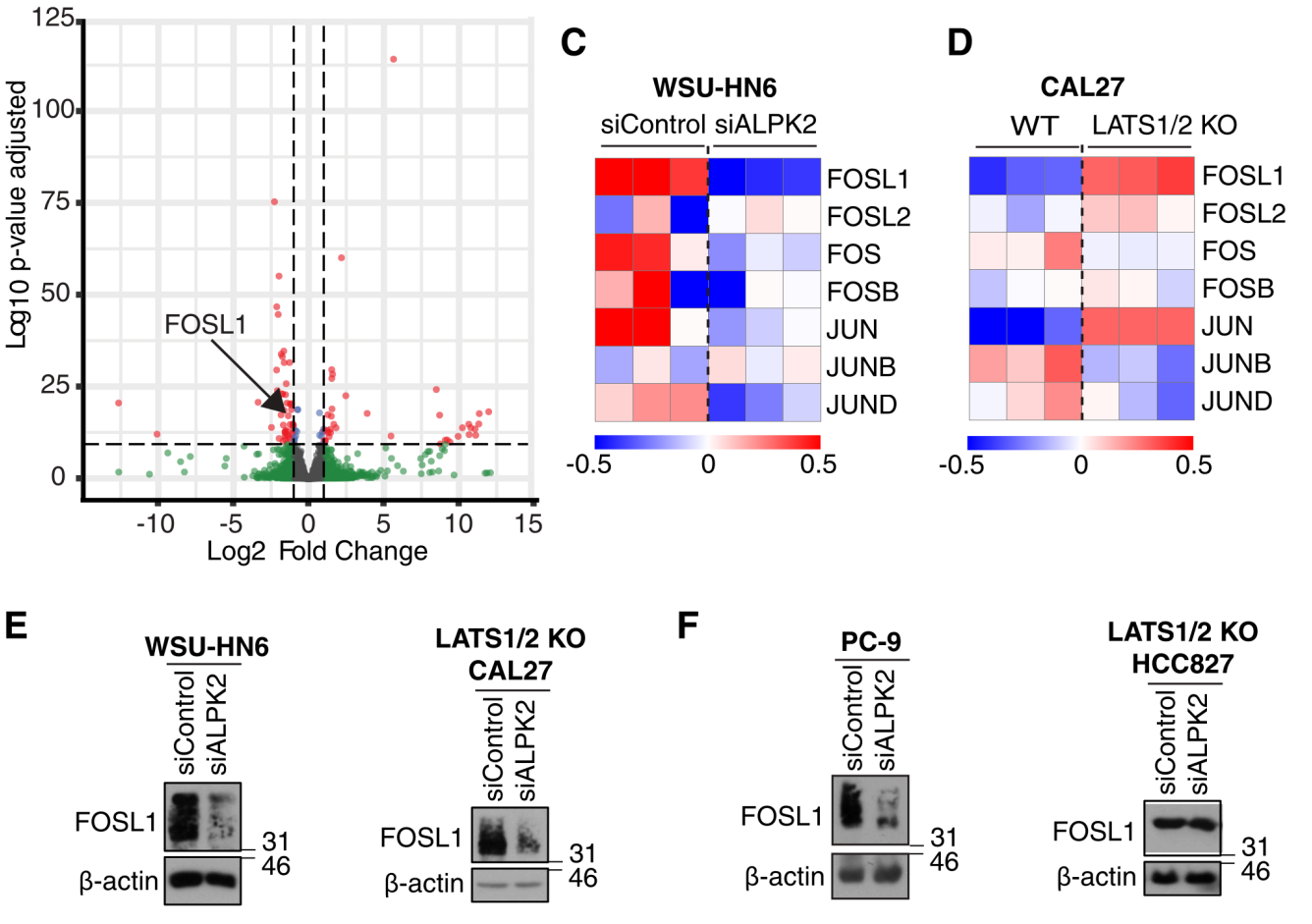


Figure 3

ALPK2 may regulate MTA2 and FOSL1

(A) Top 10 proteins with significantly decreased phosphorylation in siALPK2-transfected WSU-HN6 cells compared with siControl-transfected WSU-HN6 cells, as identified by phosphoproteomic analysis. Protein abundance is presented as iBAQ values, and statistical significance is indicated by p-values. ND,

not detected. Volcano plot of phosphoproteomic analysis following ALPK2 knockdown in WSU-HN6 cells. Proteins with |log2 fold change|>1 and adjusted P<0.05 were considered significantly differentially expressed. MTA2 is highlighted. (B) Volcano plot of RNA-seq analysis in WSU-HN6 cells following ALPK2 knockdown. Genes with adjusted P<0.05 were considered significantly differentially expressed. FOSL1 is highlighted. (C, D) Heat map showing the expression profiles of JUN and FOS family genes derived from the RNA-seq data shown in Figure 1, comparing WT and LATS1/2KO CAL27 cells. (E) Immunoblot of FOSL1 and β-actin in WSU-HN6 and LATA1/2KO CAL27 cells transfected with siControl or siALPK2. (F) Immunoblot of FOSL1 and β-actin in PC-9 cells and LATS1/2KO HCC827 cells transfected with siControl or siALPK2.

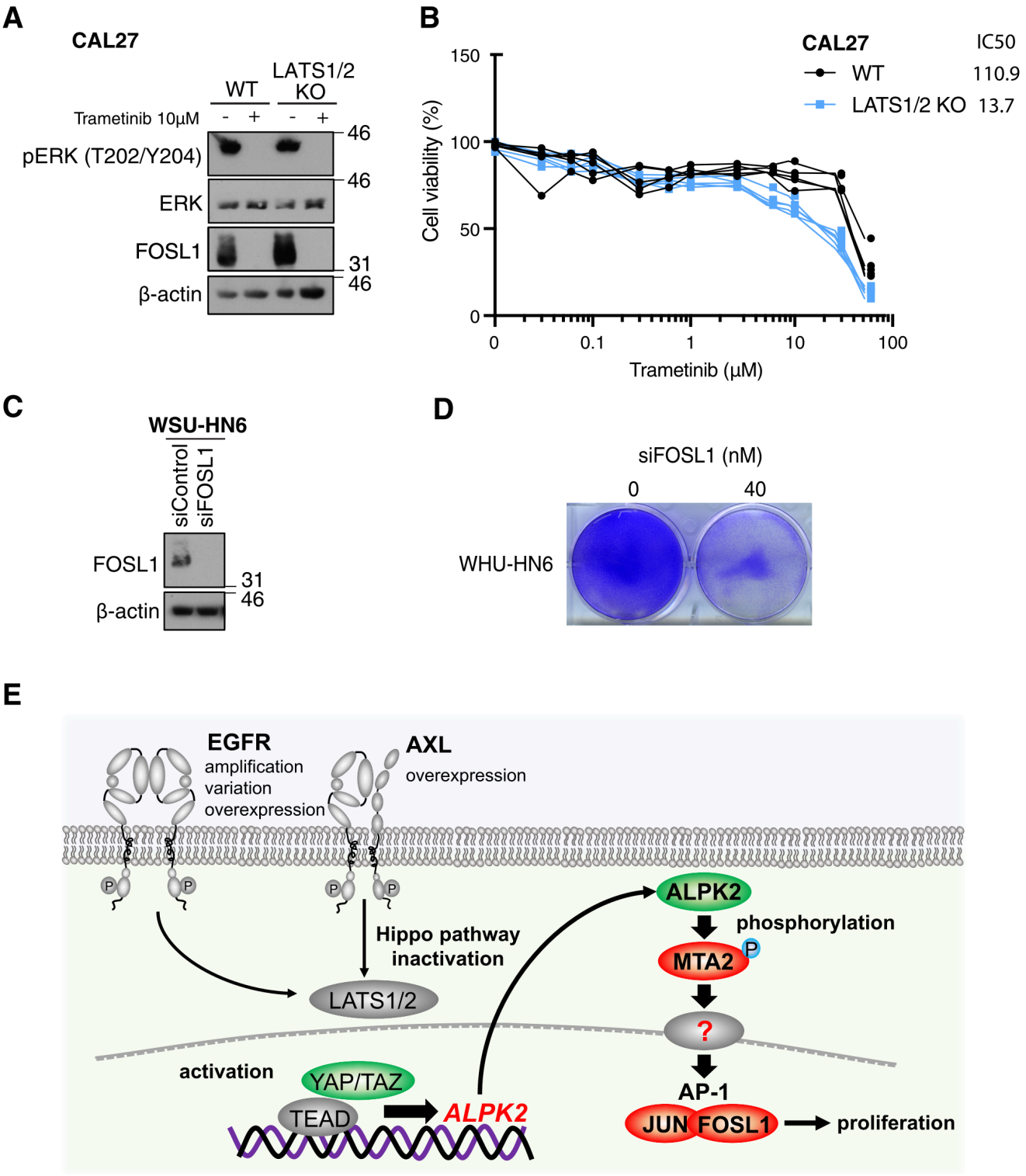


Figure 4

Trametinib suppresses the growth of YAP/TAZ-activated OSCC cells, and FOSL1 contributes to their proliferation

(A) Immunoblot of pERK, ERK, FOSL1 and β-actin in WT and LATS1/2KO CAL27 cells treated with trametinib (10 μM) or DMSO. (B) Dose–response curves showing the viability of WT and LATS1/2 KO

CAL27 cells following treatment with increasing concentrations of trametinib. Cell viability was assessed using the CellTiter-Blue assay. IC50 values were estimated by nonlinear regression using a variable-slope model. Data are presented as mean ± SD (N=5). (C) Immunoblot of FOSL1 and β-actin in WSU-HN6 cells transfected with siControl or siFOSL1. (D) Crystal violet staining of siFOSL1 or siControl in WSU-HN6 cells. (E) Summary of the mechanism. ALPK2, whose transcriptional and protein levels are increased by YAP/TAZ, phosphorylates MTA2, thereby promoting AP-1 transcription and stimulating tumor growth.

Supplementary Files

This is a list of supplementary files associated with this preprint. Click to download.

- SupplementaryFigure1.pdf
- SupplementaryFigure2.pdf
- SupplementaryFigure3.pdf